Journal of Molecular Catalysis A: Chemical 322 (2010) 33–38

Contents lists available at ScienceDirect

Journal of Molecular Catalysis A: Chemical

journal homepage: www.elsevier.com/locate/molcata

Characterization and catalytic kinetics studies of *N*-cetyl-*O*-sulfate chitosan multinuclear copper complex as an artificial hydrolase

Yan Xiang[a,*], Qi Zhang[b], Jiangju Si[a], Jianping Du[a], Hong Guo[a], Tao Zhang[b]

[a] School of Chemistry and Environment, Beihang University, Beijing, 100191, PR China
[b] School of Material Science and Engineering, Beihang University, Beijing, 100191, PR China

ARTICLE INFO

Article history:
Received 22 December 2008
Received in revised form 3 February 2010
Accepted 4 February 2010
Available online 11 February 2010

Keywords:
Chitosan
Multinuclear complex
Phosphodiester hydrolysis
Catalytic kinetics

ABSTRACT

A novel multinuclear Cu(II) complex of *N*-cetyl-*O*-sulfate-chitosan (NCOS) was prepared and structurally characterized by X-ray photoelectron spectroscopy (XPS) and Infrared radiation (IR) spectroscopy. The capability of chelated copper ions to coordinate with the novel ligand was improved 55% over native chitosan. As artificial multinuclear phosphodiesterase, NCOS-Cu(II) complex was adopted to study its catalytic kinetics on hydrolysis of bis(4-nitriphenyl)phosphate (BNPP) in the heterogeneous system. The initial rate of BNPP hydrolysis catalyzed by NCOS-Cu(II) was 7×10^4 times higher than that of spontaneous BNPP hydrolysis. The behavior of BNPP catalytic hydrolysis fits Michaelis–Menten kinetics with k_{cat} of 2.3×10^{-5} s^{-1}, the maximum velocity (V_{max}) of 2.3×10^{-9} mol L^{-1} s^{-1} and the Michaelis constant (K_M) of 2.9×10^{-4} M, respectively. The metal-hydroxyl catalytic mechanism has been proposed.

1. Introduction

Phosphodiesters are exceptionally stable, making them uniquely suited candidates to form the backbone of genetic material. Typical nucleases that catalyze the hydrolytic or nucleophilic cleavage of phosphodiesters are normally activated by metal ions and the reaction can be accelerated up to 10^{12}–10^{17} folds [1]. Therefore, it is highly important to study the biomimetic systems for the hydrolysis of phosphodiesters for not only the development of artificial restriction enzymes for molecular biology and biotechnology, but also the design of antiviral and antitumor drugs. In order to better understand possible mechanisms of how metal ions function as coenzymes to promote phosphodiester hydrolysis, researchers have examined various kinds of metal complexes and performed extensive mechanistic studies on the metal ion-promoted hydrolysis of phosphates has carried out. In those studies, large catalytic effects could be achieved solely via the metal ion-mediated direct activation. Such direct activation effects mainly including *Lewis* acid activation, intramolecular nucleophile activation and leaving group activation as well, etc. Over the past two decades, significant mimic enzyme systems for the cleavage of P–O have been constructed primely by using transition metal complexes and rare earth metal complexes [2–5]. A wide variety of interesting mononuclear, dinuclear metal complexes have been reported as structural or functional models [6–17] of phosphoesterases, such as cobalt(III) polyamine complexes [8], copper(II) complexes [9,10], zinc(II) macrocyclic polyamine complexes [6,11] and Lanthanide(III) cryptate(2.2.1) complexes [5]. Multinuclear compounds [18–20] have been reported to provide higher catalytic efficiency due to the synergistic effect between metal ions and metal ions with ligands.

As a natural polysaccharide, chitosan has distinct capability on metal ions adsorption in addition to its biocompatibility, biodegradability and bioactivity. It has been reported that some metal complexes of chitosan or its derivatives have characteristics analogous to natural enzymes; this provides strong evidence that chitosan-based compounds can be used as artificial enzyme [21]. In recent years, studies on chitosan-supported rare earth complexes used as catalyst on the polymerization of propylene oxidation have been reported [21–25]. Additionally, the catalytic capability of chitosan monomer D-glucosamine schiff-based metal complexes to PNPP hydrolysis reaction has been proved in our research group [24].

In this paper, a novel modified chitosan copper(II) complex was prepared. In order to better mimic the features of natural enzymes, long-alkyl chain and sulfate groups were, respectively, introduced on the chitosan backbone to reconstitute hydrophobic and hydrophilic microenvironment. Experimental results indicated the novel chitosan-based complex indeed exhibited remarkable catalytic capability for phosphodiester hydrolysis and suggested that the chitosan complex could be used to develop an artificial multinulear hydrolyase.

* Corresponding author at: School of Chemistry and Environment, Department of Environmental Science & Engineering, Beihang University, No. 37, Xueyuan Road, Hai Dian District, Beijing, 100191, PR China. Tel.: +86 10 82339539; fax: +86 10 82339539.
E-mail address: xiangy@buaa.edu.cn (Y. Xiang).

1381-1169/$ – see front matter © 2010 Elsevier B.V. All rights reserved.
doi:10.1016/j.molcata.2010.02.011

2. Experimental

2.1. Materials

Chitosan powder (MW: 10,000–50,000, deacetylation degree 85%, purchased from Hai De Bei. Co. Ltd. of China) was used without further purification. Cetyl chloride, chlorosulfonic acid and bis(4-nitriphenyl)phosphate (BNPP) were purchased from Aldrich. All reagents, unless indicated, were analytical grade commercial products and used without further purification. Tris–H^+ buffer was used to avoid the influence of the chemical components and its pH was adjusted by adding analytically pure hydrochloric acid in all runs. The buffer system is not sensitive to the polarity of solvent system and its pK_a changes very slightly. The substrate BNPP was prepared in acetonitrile.

2.2. Preparation of NCOS-Cu(II)

CTCS, *N*-cetyl chitosan, was prepared by the method developed by Dai et al. [26]. 1.0 g chitosan power was added into 10 ml isopropanol containing a certain amount potassium hydroxide at 40 °C under mechanical stirring for 2 h. After dropping 3–5 ml chlorocetane was added to the mixture at 60 °C, the reaction was carried out for 2–10 h. The product mixture was washed with 10 ml methanol, neutralized with diluted hydrochloric acid and deposited with acetone. The precipitate was collected by filtration and dried in air after successive washing by acetone and ether. The fine CTCS was obtained after dialysis in deionized water for 24 h. CTCS is water insoluble.

The ligand NCOS, *N*-cetyl-*O*-sulfated chitosan, was synthesized by 6-*O*-sulfation of *N*-cetyl chitosan according to the literature method [27]. CTCS (1.0 g) was suspended in dimethylformamide (DMF) (40 ml) by stirring. Chlorosulfonic acid (20 ml) was added into DMF at 0 °C. The mixture was stirred for 24 h at room temperature. Next, the solution was neutralized with 10 mM sodium hydroxide. The filtered solution was dialyzed against distilled water and then lyophilized, and the NCOS powder was obtained.

Certain amount of NCOS powder was homogeneously dispersed in a flask by ultrasonic dispersion. Then 1% copper chloride solution was added into the reaction vessel. The mixed solution was stirred continuously for 4 h at 50 °C, deposited by acetone and intensively washed with distilled water. The crude product was vacuum-dried and recrystallized with methanol. Both the ligand NCOS and the final product NCOS-Cu are water-insoluble products.

2.3. Characterization

Elemental analysis was determined by using an Element Vario EL III analyzer. Anal. Calc. for chitosan (wt%): C: 33.06; H: 6.75; N: 6.29; Anal. Calc. for NCOS (wt%): C: 40.64; H: 5.73; N: 3.92; S: 10.85. On the basis of the elemental analysis, we estimated that alkylation degree and sulfonation degree of NCOS were 40.76% and 48.44%, respectively; see Eqs. (1) and (2).

$$\text{Cetylation}\,(\%) = \frac{\Delta m_c/12n_c}{N\%/14} \times 100 = 40.76 \quad (1)$$

$$\text{Sulfonation}\,(\%) = \frac{10.85/\text{Mso}_3^{2-}}{3.92/14} \times 100 = 48.44 \quad (2)$$

Inductively coupled plasma atomic emission spectrometry (ICP-AES) was performed by using IRIS Intrepid IIXSP to determine the content of copper ions in the complexes. The parameters are as follows: RF power: 1150 W; nebulizer flow: 26.0 PSI; auxiliary gas: 1.0 LPM. The copper content of the unmodified chitosan copper complex prepared in our lab was 2.8% and that of NCOS-Cu(II) was 4.4%, indicating a 55% improvement.

X-ray photoelectron spectroscopy of NCOS and NCOS-Cu(II) were recorded by using an X-ray Photoelectron Spectrometer (VG Scientific Escalab 210-UK) equipped with a twin anode (Mg K/Al K) source. The samples were placed in a vacuum in the range 10^{-8} to 10^{-7} Pa and the analyzed sample area was Ø6 μm to Ø6 mm. The scanning condition was 6.80 ms/step, 0.6 eV/step and 6 sweeps.

Fourier transform infrared spectra (FTIR) were obtained with a Perkin-Elmer FTIR 1600 series spectrometer by using KBr discs.

2.4. Catalytic kinetics study

Due to the limited solubility of NCOS-Cu(II) complex in Tris–H^+ buffer, kinetic measurement was carried out under heterogeneous condition by adding complex into the continuously stirred reaction system with the fixed concentration of BNPP. The concentration of the catalyst [NCOS-Cu(II)] was calculated by using Eq. (3), where the copper content in the complex was calculated according to the results of ICP-AES (m is the quality of the complex used in the reaction; V_0 is the volume of reaction solution).

$$[\text{NCOS-Cu(II)}] = \frac{m \times \text{Cu}\%}{63.5\,V_0} \quad (3)$$

Every 15 min, 3 ml samples were drawed from the reaction system and filtered with ultrafiltration membrane (aperture 22 μm), then the clear liquid was used for measuring absorbance. The change in absorbance at 400 nm, which represents the release of *p*-nitrophenolate anion from BNPP, was recorded and the data were processed to obtain the initial rate plots. All runs were conducted in triplicate, from which standard deviations of typically 2–5% were obtained, as indicated by error bars in the data plots. Curve fitting of the saturation kinetics was performed by using OriginPro 7.5 (Microcal) software.

3. Results and discussion

3.1. IR analysis

The IR spectra of Chitosan, NCOS and the Copper complex of NCOS are shown in Fig. 1. The Fit Multi-peaks function of OriginPro7.5 was used to analyze the overlapping peak.

The IR spectrum of *N*-cetyl-*O*-sulfate chitosan showed differences at 1633–1527 cm^{-1}, 1160–1040 cm^{-1}, 2831–2925 cm^{-1} and 1290–1236 cm^{-1} these differences correspond to the vibration of N–H [26], –OH, $-CH_3$ and –S=O [26,27], respectively. All these

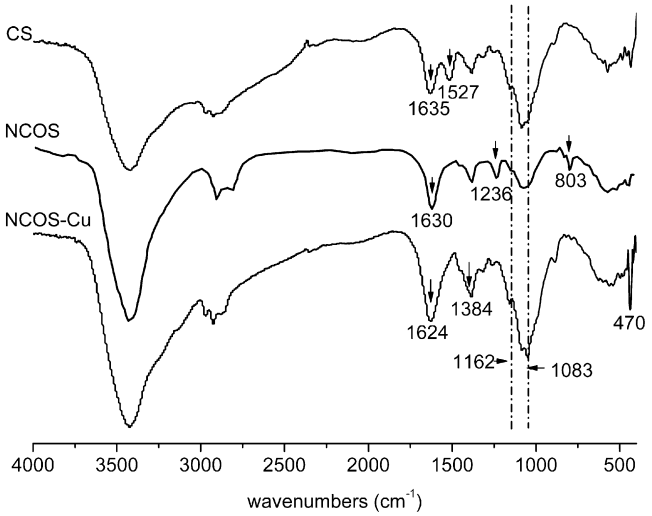

Fig. 1. IR spectra of chitosan and chitosan derivatives.

Table 1
Electron binding energy of O_{1s}, N_{1s} and Cu_{2p}.

Samples[a]	O_{1s}	N_{1s}	$Cu_{2p_{1/2}}$	$Cu_{2p_{3/2}}$
1	–	–	954.2	934.2 [29]
2	531.6	398.6	–	–
	531.1			
3	531.7	400.5	–	–
	531.1	398.5		
4	532.9	401.8	952.8	932.9
	532.0	399.7		

[a] 1. $CuCl_2{\cdot}2H_2O$; 2. CTCS; 3. NCOS; 4. NCOS-Cu.

changes revealed the successful introduction of the long-alkyl chain and sulfonic group.

For NCOS-Cu(II) complex, the wide adsorption band at 3442 cm^{-1}, corresponding to the vibration of amino group and hydroxyl group, shifted down to 3421 cm^{-1}, and the adsorption peak of N–H twisting at 1630 cm^{-1} also moved down to 1624 cm^{-1} which indicated both amino and hydroxyl groups were involved in complexation with copper ion. This is in agreement with the new band at 470 cm^{-1}, corresponding to stretching vibration of Cu–N [28].

3.2. XPS analysis

The XPS full scan of NCOS-Cu(II) in Fig. 2 shows the presence of the sulfur element in the complex, which confirms the successful sulfonation on chitosan backbone. The electron binding energy of N, O, and Cu^{2+} in different compounds was detected and is listed in Table 1, respectively. As shown in Fig. 3, the new peak of N_{1s} can be observed both in NCOS ligand and its complex, For the *N*-cetylchitosan, the nitrogen binding energy was found mainly distributes at 398.6 eV which can be separated into different energy peaks by curve fitting [29]. We proposed here that there were at least two kinds of nitrogen atoms in CTCS and NCOS with binding energies of 398.5 and 400.5 eV, respectively. The higher energy peak at 400.5 eV can be assigned to certain N atoms that become more active due to the introduction of electrophilic sulfuric groups. In contrast, the two different nitrogen environments of NCOS-Cu(II) showed increased binding energies of 401.8 eV [30–33] and 399.5 eV, respectively, suggesting that they were in the different chemical conformation, possibly related to the coordination of Cu(II) ions. The O_{1s} binding energy for CTCS and NCOS was around 531.5 eV; as shown in Fig. 4. The O_{1s} spectra of NCOS-Cu(II) complex also displayed an up-shifted peak at 532.7 eV,

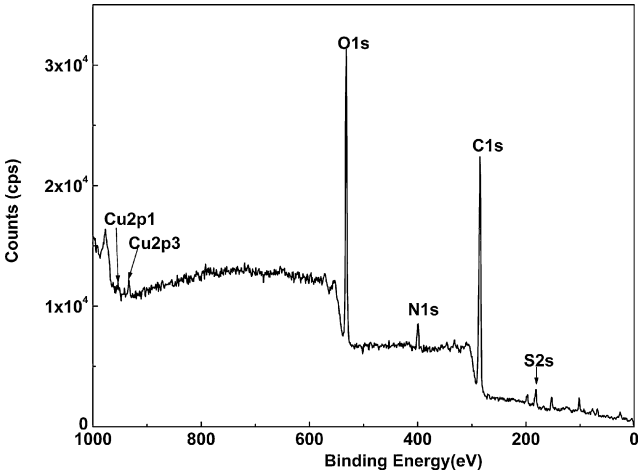

Fig. 2. XPS full scan spectrum of NCOS-Cu(II) complex.

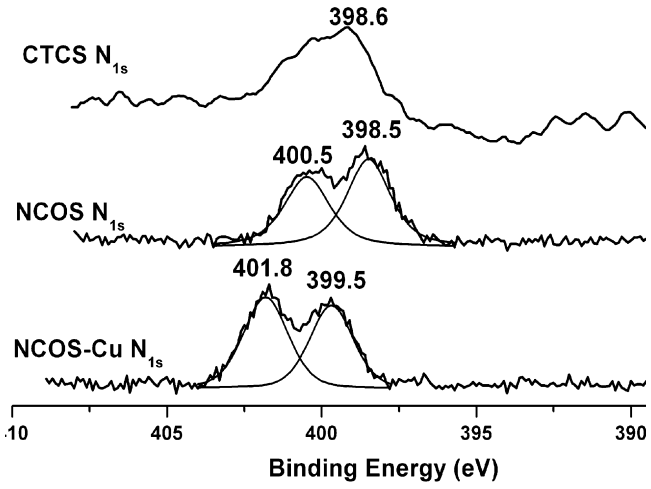

Fig. 3. XPS N_{1s} spectra of NCOS-Cu(II) complex.

suggesting the activation of O atoms by the complexation process [34].

Two sharp peaks for Cu(II) were observed in $2p_{3/2}$ and $2p_{1/2}$ orbits existed in NCOS-Cu(II) with the binding energy of 932.9 eV ($Cu_{2p_{3/2}}$) and 952.8 eV ($Cu_{2p_{1/2}}$) (Fig. 5). Unlike the binding energy of the copper chloride salt, that of Cu(II) in NCOS-Cu showed a markedly decrease by 1.4 eV for $Cu_{2p_{3/2}}$ and 1.3 eV for $Cu_{2p_{1/2}}$. Additionally, the shake-up effect was not observed, suggesting that all the Cu(II) ions in the complex were chelated. Therefore significant energy changes were observed on N_{1s}, O_{1s} and Cu_{2p} in NCOS-Cu(II),

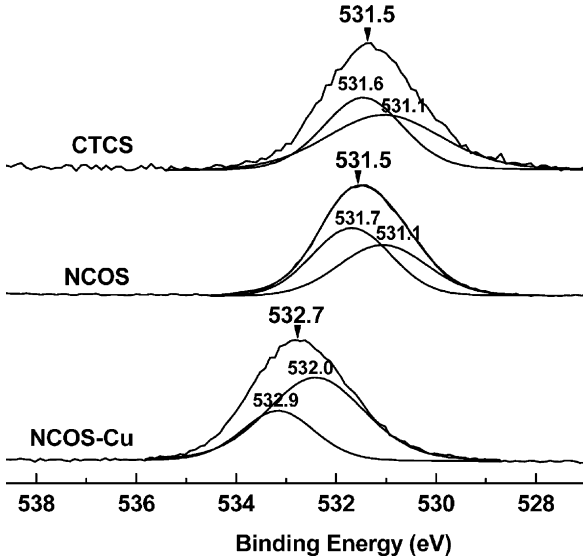

Fig. 4. XPS O_{1s} spectra of CTCS, NCOS and NCOS-Cu(II).

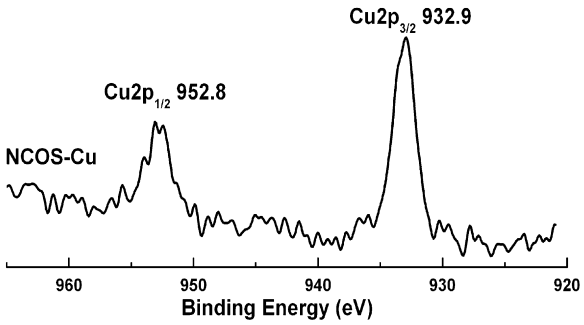

Fig. 5. XPS Cu_{2p} spectra of NCOS-Cu.

indicating that their electron states were possibly responsible for the coordination. There was a concomitant increase in the binding energy of N_{1s} and O_{1s} with the decrease in binding energy of Cu_{2p} around 1.3 eV, this proportionate energy variation might suggest possibility of electron transfer from nitrogen and oxygen atoms to the copper ions. There was a great probability that the coordination bonds formed between the nitrogen atom, oxygen atom and copper ions using the dsp^2 hybrid orbits. In chitosan, the 6-, and 3-hydroxyl groups are more active for interacting with copper ions but because the 6-hydroxyl group is sulfonated in N-cetyl-O-sulfate chitosan, the copper ion most probably coordinates with the 3-O atoms. It is proposed that copper ions exist in the tetra-coordinate state during complexation in NCOS-Cu(II), as depicted in Scheme 1.

3.3. Catalytic kinetic studies

3.3.1. Apparent rate constants for hydrolysis of BNPP

The model substrate, phosphodiester substrate bis-(p-nitrophenyl)phosphate (BNPP), was used to evaluate the efficiency and specificity of the complexes for the hydrolysis of phosphodiester bonds. Generally, although metal complex-promoted hydrolysis of phosphate diesters is a slow reaction, its kinetics can be studied by the method of initial rates [35,36].

The observed rate constant k_{obs} of spontaneous hydrolysis of BNPP was reported as $1.1 \times 10^{-11}\ s^{-1}$ at pH = 7 at room temperature [37]. With our catalysts, all catalytic reactions occurred at an increased rate. As data shown in Table 2, the metal ions and Tris–H^+ buffer exhibited a certain positive effect on the BNPP hydrolysis. The k_{obs} of $4.8 \times 10^{-11}\ s^{-1}$ was obtained for BNPP hydrolysis in Tris–H^+. Slight rate-acceleration was found when copper ions were used alone or when unmodified chitosan catalytic system was used. In contrast, remarkable acceleration up to the order of 4×10^4-fold

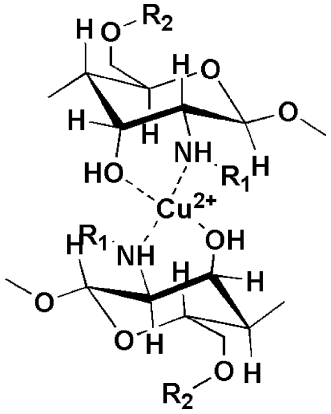

Scheme 1. Proposed coordination form of Cu^{2+} in the complexes. R1 is long-alkyl chain, R2 is sulfonic group. Copper ions existed in the form of tetra-coordinated state in NCOS-Cu(II).

Table 2
Pseudo rate constants for the hydrolysis of BNPP[a].

Entry	System	k_{obs} (s^{-1})
1	Spontaneous hydrolysis [37]	1.1×10^{-11}
2	Tris–H^+ buffer	4.8×10^{-11}
3	Cu^{2+}/Tris–H^+	7.4×10^{-11}
4	CS/Tris–H^+	7.1×10^{-11}
5	NCOS-Cu/Tris–H^+	4.7×10^{-7}

[a] The reactions were carried out in Tris–H^+ at pH 8.0, 25 °C. [BNPP] = 0.05 mM, [Cu^{2+}] = 0.1 mM.

of that of spontaneous hydrolysis of BNPP was achieved by NCOS-Cu(II) in Tris-H^+ buffer. These results indicated the fine catalytic capability of NCOS-Cu(II) complex on BNPP hydrolysis.

3.3.2. Effect of pH values on the rate of BNPP hydrolysis

The effect of pH on the reaction rate was determined and correlated with the pK_a of coordinated water molecular in NCOS-Cu(II). Kinetic experiments were performed in Tris–H^+ at pH varying from 6.9 to 9.0 with a fixed concentration of BNPP (0.05 mM). The pH-V_0 profile for NCOS-Cu promoted hydrolysis of BNPP was a bell-shaped curve as shown in Fig. 6 with a maximum at pH 8.0. That indicated the catalytic mechanism of NCOS-Cu(II) involved a metal-hydroxyl nucleophilic attack [35–37]. The pK_a value of the copper-bound water molecules in NCOS-Cu was approximately 7.9. The maximum of the rate of BNPP hydrolysis catalyzed by NCOS-Cu can be achieved at pH ~ 8, when the copper complex was formed in the aqua hydroxyl active species [35–37].

The process of BNPP hydrolysis catalyzed by NCOS-Cu(II) can be described as follows: first, the catalyst probably forms an intracomplex with substrate, and the association constant of this complex was k_1 and k_{-1} (Eq. (4)) [38,39]. In this equation, the rate constant k_{-1} was neglected to simplify the calculation. Next, the intramolecular nucleophilic reaction occurs via the phosphorus atom at a rate constant k_2 to form the products (Eq. (5)) [40]. Eq. (5) was considered to be the rate-limited step since $k_2 \ll k_1$. On the basis of the rate equation (Eq. (6)), the pseudo rate constant k_{obs} can be expressed as Eq. (7); in this equation, [S] is the initial concentration of BNPP. The rate equations can also be expressed as the Michaelis–Menten equation format or as the Lineweaver–Burke format, as shown in Eqs. (8) and (9), respectively, where $K_M = k_2/k_1$ ($k_2 \ll k_1$).

$$[\text{NCOS-Cu}] + {}^{-}\text{OPO(OR)(OR}') \underset{k_{-1}}{\overset{k_1}{\rightleftharpoons}} [\text{NCOS-Cu-OPO(OR)(OR}')] \qquad (4)$$

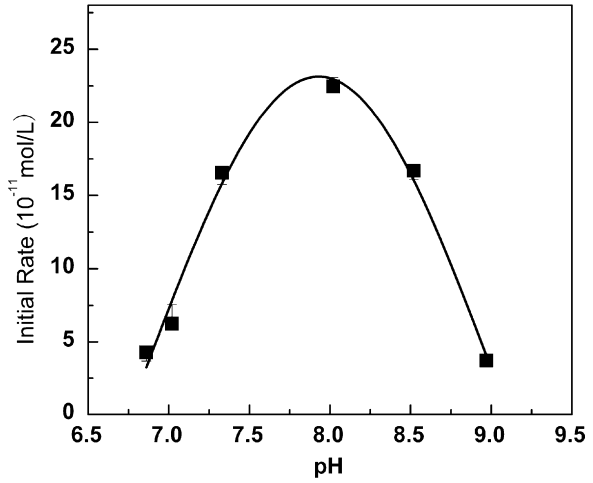

Fig. 6. pH-rate profiles for the BNPP hydrolysis catalyzed by NCOS-Cu(II) in Tris–H^+ buffer at 25 °C, [BNPP] = 0.05 mM, [NCOS-Cu(II)] = 0.1 mM. The pK_a of the copper-bound water molecule is 7.9.

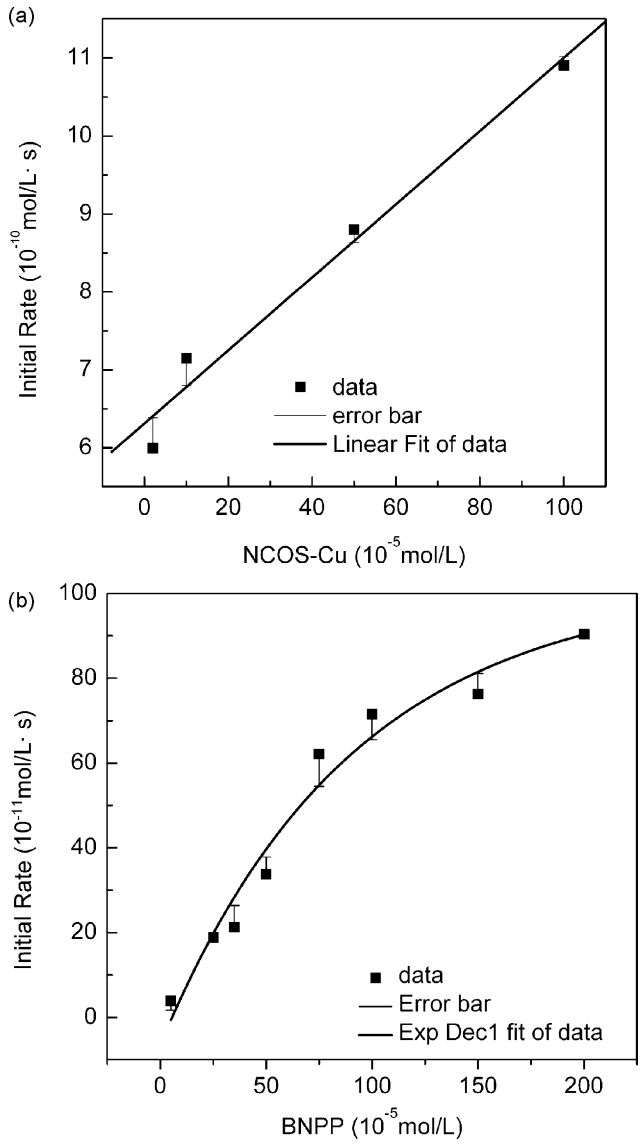

Fig. 7. Dependence of initial rate on the concentration of NCOS-Cu(II) and BNPP. For (a) [BNPP] = 1 mM, [NCOS-Cu(II)] = 0.02–1 mM. The plotted line fits to the data for which $R > 0.99$. Saturation kinetics of NCOS-Cu by BNPP was shown in (b), [BNPP] = 0.05–2 mM, [NCOS-Cu(II)] = 0.1 mM [Tris–H^+] = 10 mM. The lines were plotted with least-square method and fitted well with $R^2 = 0.99$. All the tests were going under the condition of pH = 8.0, $T = 25\,^\circ$C.

$$[\text{NCOS-Cu-OPO(OR)(OR}')] \xrightarrow{k_2} {}^{-}\text{OR} + {}^{2-}\text{OPO}_2(\text{OR}') + [\text{NCOS-Cu}] \quad (5)$$

$$v = \frac{d[\text{OR}]}{dt} = k_1 k_2 [\text{NCOS-Cu}][{}^{-}\text{OPO(OR)(OR}')] = k_{obs}[\text{S}] \quad (6)$$

$$k_{obs} = k_1 k_2 [\text{NCOS-Cu}] \quad (7)$$

$$v = \frac{V_{\max}[\text{S}]}{K_M + [\text{S}]} \quad (8)$$

$$\frac{1}{V} = \frac{1}{V_{\max}} + \frac{K_M}{V_{\max}} \times \frac{1}{[\text{S}]} \quad (9)$$

In our experiments, the catalysts have been adopted in a relatively large range equivalent of 2×10^{-5} to 1×10^{-3} mol/l (Fig. 7a) with 1 mM BNPP in our experiments. As shown in Fig. 7a, the initial rate was linearly dependent on the concentration of NCOS-Cu(II). With a fixed catalyst concentration, the hydrolytic rates fitted the first-order reaction kinetic at lower BNPP concentration but exhibited a saturation trend at higher substrate concentration, indicating that

Table 3
Calculated initial rates V_0 and observed rate constant k_{obs} for BNPP hydrolysis[a].

Concentration of substrate ($\times 10^{-5}$ mol/l)	Initial Rate ($\times 10^{-11}$ mol/l s)	k_{obs} ($\times 10^{-5}$ s^{-1})	R^2
5	3.9	2.31	0.97
25	18.8	2.36	0.99
35	21.2	1.97	0.98
50	32.8	2.23	0.99
75	65.1	3.17	0.98
100	71.5	2.79	0.98
150	76.3	2.24	0.99
200	90.4	2.21	0.99

[a] [NCOS-Cu(II)] = 0.1 mM; the reactions were carried out in Tris–H^+ buffer at pH 8.0. The initial rate was calculated by non-linear fitting of the absorbency data.

they satisfied the Michaelis–Menten behavior (Fig. 7b). The experimental data (listed in Table 3) also showed a good fit with the Lineweaver–Burke function well and resulted in a precise straight line, as shown in Fig. 8. According to Eq. (9), the Michaelis–Menten parameters K_M was calculated at 2.9×10^{-3} M, and the maximum reaction rate V_{max} was calculated at 2.3×10^{-9} mol L^{-1} s^{-1}. The turnover number k_{cat} for BNPP hydrolysis was 2.3×10^{-5} s^{-1}. On the basis of Eq. (7) and K_M, the rate constant k_1 and k_2 were calculated at 2.6 s^{-1} and 7.5×10^{-3} s^{-1}, respectively; those results are consistent with our hypothetical conditions of $k_2 \ll k_1$ and rate-determining step of Eq. (5). All the above results indicated the validity of our proposed kinetics model.

Generally, the enzymatic activity depends upon the acidity of a reaction system and the protonation states of complexes. In a reaction process, polar interaction such as hydrogen bonding and dipole–dipole interactions, as well as electrostatic interactions, between the catalyst and the substrate contributes significantly to the catalytic efficiency [41,42]. In the NCOS-Cu(II) catalyzed system, the deliberate introduction of the long-alkyl chain enabled the construction of an artificial hydrophobic microenvironment as an active center with the enhanced polarity in the active sites, which could largely improve the activity of the active species and the attractiveness toward the substrate. Hence the NCOS-Cu(II)-BNPP intracomplex could easily form in the catalytic system, which is indicated by the calculated k_1 value. The bell-shaped pH-rate profile can be explained by assuming that each metal ion binds a water molecule, thereby deprotonating it; this provides a stronger base under a particular pH range. The efficiency of the catalytic activity might be reduced by the flocculation of copper ions from the complex in a relatively strong alkaline solution.

We have demonstrated that Cu(II) ions are tetra-coordinated in the complexes. This can be speculated based on the specific structure of NCOS that provides both hydrophobic and hydrophilic microenvironment, thereby enhancing the reactivity of the NCOS-

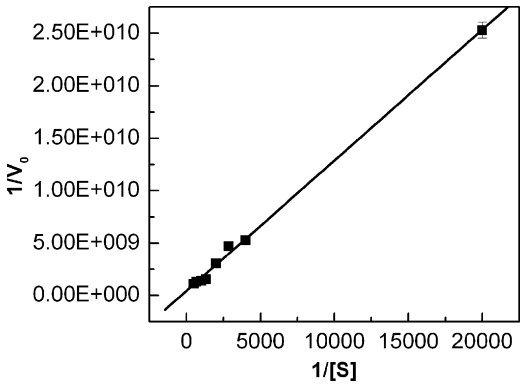

Fig. 8. Lineweaver–Burk plots for BNPP hydrolysis. [NCOS-Cu(II)] = 0.1 mM, [Tris–H^+] = 10 mM. $K_M = 2.9$ mM and $k_{cat} = 2.3 \times 10^{-5}$ s^{-1}, $R = 0.99$.

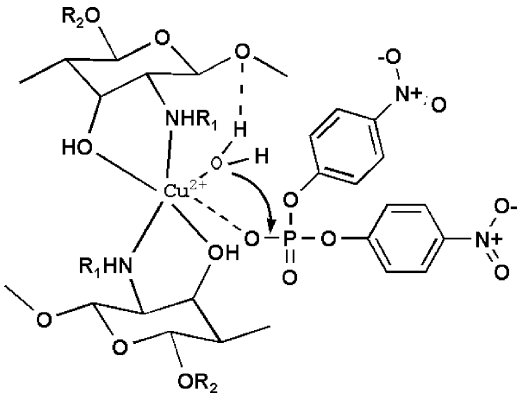

Scheme 2. Proposed mechanism of NCOS-Cu(II) catalysis. In reaction system, Cu(II) in NCOS-Cu(II) is considered as the active center of the catalysis system. The metal-hydroxide associates with substrate to realize the formation of intermediate.

Cu(II) complex for the hydrolysis of phosphodiester bonds, and the Cu(II) ions can contribute to catalytic procedure as described in Scheme 2. Copper ions mainly acted as strong *Lewis* acid for the activation of the phosphodiester bonds and the generation of nucleophiles [40,41]. With the support of electrostatic stabilization between Cu(II) ions and coordinated hydroxyl ions as well as alkaline environment, the Cu(II)-bound hydroxyl groups are able to interact more actively. For BNPP, the activation of Cu(II) induced the phosphorus atoms to become more electrophilic, thereby making them more susceptible toward anionic nucleophiles. Subsequently, the approach of the nucleophile and the release of the leaving group occur in turns. Taken together, the hydrolysis reaction of BNPP catalyzed by NCOS-Cu(II) complex is supposed to be a metal-hydroxyl nucleophilic mechanism that is based on a complicated multinuclear polysaccharide complex.

4. Conclusions

N-cetyl-*O*-sulfated chitosan copper(II) multinuclear complex was prepared and characterized. Based on IR and XPS results, we demonstrated that tetra-coordination bonds formed between Cu(II) and 2-amide *N*, 3-hydroxyl *O* of the ligand NCOS using the dsp^2 hybrid orbital. The amount of chelated Cu(II) in the NCOS-Cu(II) complex was 55% more than that in the native chitosan. As a catalyst for the hydrolysis of phosphodiester bonds in BNPP, the NCOS-Cu(II) complex presented a distinct catalytic capability with 7×10^4 times rate-acceleration compared to BNPP spontaneous hydrolysis. The multinuclear catalytic kinetics model was proposed, and the catalytic behaviors fitted well. The kinetics parameters derived from the hydrolysis reaction were very helpful for understanding the catalysis process. The metal-hydroxyl nucleophilic mechanism was suggested where copper ions acted as strong *Lewis* acid for the activation of the phosphodiester bonds and the generation of nucleophiles.

Acknowledgement

This work was supported by the National Nature Science Foundation of China (Grant 20403002, 20773008).

References

[1] E.H. Serpersu, D. Shortle, A.S. Mildvan, Biochemistry 26 (1987) 1289–1300.
[2] Q. Liu, H.M. Chen, H. Lin, J. Mol. Catal. A: Chem. 269 (2007) 104–109.
[3] F. Aguilar-Perez, P. GomezTagle, E. Collado-Fregoso, A.K. Yatsimirsky, Inorg. Chem. 45 (2006) 9502–9517.
[4] E.R. Farquhar, J.P. Richard, J.R. Morrow, Inorg. Chem. 46 (2007) 7169–7177.
[5] S.J. Oh, K.H. Song, D. Whang, Inorg. Chem. 35 (1996) 3780–3785.
[6] F. Mancin, E. Rampazzo, P. Tecilla, U. Tonellato, Eur. J. Org. Chem. (2004) 281–288.
[7] D.Y. Kong, A.E. Martell, J. Reibenspies, Inorg. Chim. Acta 333 (2002) 7–14.
[8] T. Gunnlaugsson, M. Nieuwenhuyzen, C. Nolan, Polyhedron 22 (2003) 3231–3242.
[9] F.B. Jiang, L.Y. Huang, X.G. Meng, J. Colloid Interface Sci. 303 (2006) 236–242.
[10] K. Selmeczi, M. Giorgi, G. Speier, Eur. J. Inorg. Chem. (2006) 1022–1031.
[11] M. Shionoya, E. Kimura, M. Shirot, J. Am. Chem. Soc. 115 (1993) 6730–6736.
[12] K.A. Deal, G. Park, J.L. Shao, Inorg. Chem. 40 (2001) 4176–4182.
[13] K.A. Deal, J.N. Burstyn, Inorg. Chem. 35 (1996) 2792–2798.
[14] T. Gajda, R. Kramer, A. Jancso, Eur. J. Inorg. Chem. (2000) 1635–1644.
[15] B.Y. Jiang, Y. Xiang, J. Du, Colloids Surf. A 235 (2004) 145–151.
[16] R. Cacciapaglia, A. Casnati, L. Mandolini, J. Am. Chem. Soc. 129 (2007) 12512–12520.
[17] R. Cacciapaglia, A. Casnati, L. Mandolini, J. Am. Chem. Soc. 128 (2006) 12322–12330.
[18] Y. Xiang, X.C. Zeng, S.Q. Cheng, J. Colloid Interface Sci. 235 (2001) 114–118.
[19] S.Q. Cheng, Y.R. Wang, J.F. Yan, Colloids Surf. A 292 (2007) 32–35.
[20] P. Scrimin, P. Tecilla, U. Tonellato, Colloids Surf. A 144 (1998) 71–79.
[21] A.V. Kucherov, N.V. Kramareva, E.D. Finashina, J. Mol. Catal A: Chem. 198 (2003) 377–389.
[22] D.J. Macquarrie, J.J.E. Hardy, Ind. Eng. Chem. Res. 44 (2005) 8499–8520.
[23] X.B. Zeng, Y.F. Zhang, Z.Q. Shen, J. Polym. Sci. Part A: Polym. Chem. 35 (1997) 2177–2182.
[24] S.X. Li, R.L. Liu, Y. Xiang, X.C. Zeng, J. Sichuan Univ. (Natural Science Edition) 39 (2002) 1089–1093.
[25] T. Vincent, S. Spinelli, E. Guibal, Ind. Eng. Chem. Res. 2003 (2003) 5968–5976.
[26] Z. Dai, D.-X. Sun, Y. Guo, Modern Chem. Ind. (Chin.) 22 (2002) 22–25.
[27] C. Zhang, Q. Ping, H. Zhang, J. Shen, Carbohydr. Polym. 54 (2003) 137–141.
[28] S.L. Sun, A.Q. Wang, J. Hazard. Mater. 131 (2006) 103–111.
[29] Y.C. Su, H. Guan, Acta Chim. Sin. 57 (1999) 596–602.
[30] H.Y. Chen, L. Chen, J. Lin, K.L. Tan, Inorg. Chem. 36 (1997) 1417–1423.
[31] D.H. Kim, W.H. Jo, Macromolecules 33 (2000) 3050–3058.
[32] G. Lawrie, I. Keen, B. Drew, Biomacromolecules 8 (2007) 2533–2541.
[33] H.J. Martin, K.H. Schulz, Langmuir 23 (2007) 6645–6651.
[34] S.K. Tama, J. Dusseault, S. Polizua, Biomaterials 26 (2005) 6950–6961.
[35] J. Chin, Curr. Opin. Chem. Biol. 1 (1997) 514–521.
[36] J. Chin, Acc. Chem. Res. 24 (1991) 145–152.
[37] F.B. Jiang, J. Du, X.Q. Yu, J. Colloid Interface Sci. 273 (2004) 497–504.
[38] J.H. Kim, J. Chin, J. Am. Chem. Soc. 114 (1992) 9792–9795.
[39] J.R. Morrow, W.C. Trogler, Inorg. Chem. 27 (1988) 3387–3394.
[40] J.N. Burstyn, K.A. Deal, Inorg. Chem. 32 (1993) 3585–3586.
[41] T. Klabunde, N. Strater, R. Frohlich, J. Mol. Biol. 259 (1996) 737–748.
[42] A. O'Donoghue, S.Y. Pyun, M.Y. Yang, J. Am. Chem. Soc. 128 (2006) 1615–1621.